JACS
JOURNAL OF THE AMERICAN CHEMICAL SOCIETY
pubs.acs.org/JACS
Communication

Synthesis and Characterization of a Bridging Cerium(IV) Nitride Complex

Henry H. Wilson, Xiaojuan Yu,[‖] Thibault Cheisson,[‖] Patrick W. Smith, Pragati Pandey, Patrick J. Carroll, Stefan G. Minasian,* Jochen Autschbach,* and Eric J. Schelter*

Cite This: *J. Am. Chem. Soc.* 2023, 145, 781−786

ABSTRACT: Complexes featuring lanthanide−ligand multiple bonds are rare and highly reactive. They are important synthetic targets to understand 4f/5d-bonding in comparison to d-block and actinide congeners. Herein, the isolation and characterization of a bridging cerium(IV)-nitride complex: $[(TriNOx)Ce(Li_2\mu\text{-}N)Ce(TriNOx)][BAr^F{}_4]$ is reported, the first example of a molecular cerium-nitride. The compound was isolated by deprotonating a monometallic cerium(IV)-ammonia complex: $[Ce^{IV}(NH_3)(TriNOx)][BAr^F{}_4]$. The average Ce═N bond length of $[(TriNOx)Ce(Li_2\mu\text{-}N)Ce(TriNOx)][BAr^F{}_4]$ was 2.117(3) Å. Vibrational studies of the ^{15}N-isotopomer exhibited a shift of the Ce═N═Ce asymmetric stretch from ν = 644 cm^{-1} to 640 cm^{-1}, and X-ray spectroscopic studies confirm the +4 oxidation state of cerium. Computational analyses showed strong involvement of the cerium 4f shell in bonding with overall 16% and 11% cerium weight in the σ- and π-bonds of the Ce═N═Ce fragment, respectively.

The isolation of novel metal-nitrido complexes continues to be an important goal, due to their relevance to N_2 fixation and importance of understanding their nucleophilic or electrophilic reactivity characteristics and associated electronic structures.[1] Molecular actinide nitrides (Scheme 1) have received significant attention in these contexts and as molecular probes to study metal−ligand multiple bonding and covalency.[2] For example, Hayton, Cho, and Autschbach recently pioneered the use of solid state ^{15}N NMR spectroscopy for the study of actinide-ligand covalency in $[K(18\text{-crown-6})(THF)_2][((SiMe_3)_2N)_3Th(\mu\text{-}N)Th(N(SiMe_3)_2)_3]$- (Scheme 1).[3] While the actinides have seen the development of a library of such compounds, examples of lanthanide nitride complexes remain scarce.[2a,b,e,4]

Scheme 1. Select, Reported Imido- and Nitride-Complexes of f-Elements

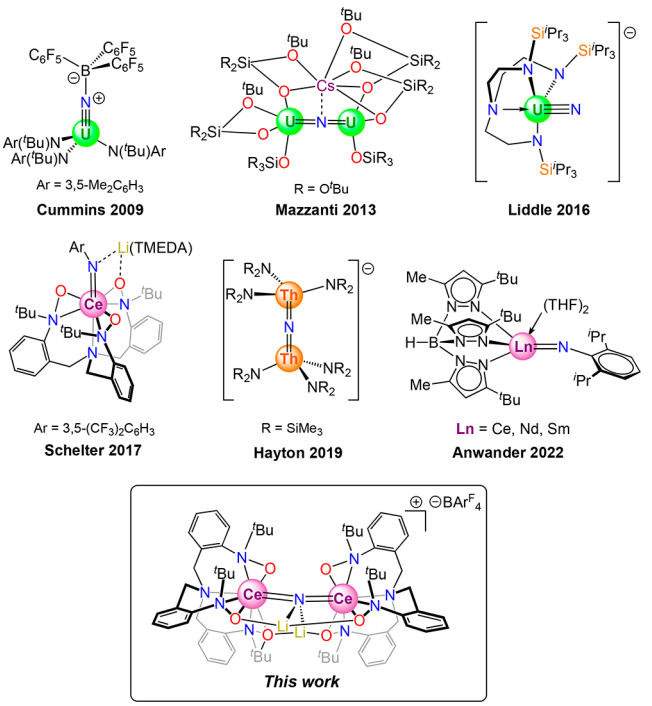

Lanthanide-nitride complexes are elusive, owing to the reactive nature of these metal−ligand multiple bonds.[2d,5] Poor spatial overlap and energy mismatch between the valence metal- and ligand-orbitals results in polarized, reactive bonds, promoting decomposition.[6] Reported examples include endohedral metallofullerenes, such as $Ce_2M_2N@C_{80}$ M = Sc, Y, Lu stabilized by encapsulation,[7] and spectroscopic studies of gas phase ions comprising Ln≡N moieties.[8] It is of interest to isolate molecular examples of lanthanide-nitride complexes to study differences in electronic structure and reactivity between d-block, actinide, and lanthanide congeners. Our work in developing the chemistry of lanthanide-ligand multiple bonds has focused on stabilizing the cerium(IV) ion, which includes bonding contributions from metal 4f- and 5d-orbitals and affords comparison with uranium(IV) and thorium(IV) compounds, and group IV metals.[3,9] Moreover, some formally cerium(IV) complexes that include noninnocent ligands have demonstrated unusual electronic structures including multiconfigurational ground states, the hallmark example being

Received: November 15, 2022
Published: January 5, 2023

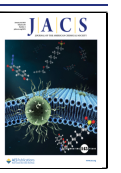

https://doi.org/10.1021/jacs.2c12145
J. Am. Chem. Soc. 2023, 145, 781−786

cerocene.[10] As such, a molecular cerium(IV)-nitride target presents an opportunity to study the electronic structure of the cerium-nitride fragment with the potential for valence ambiguity.

Previously, the coordination chemistry of the tripodal, anionic hydroxylaminato ligand framework $[\{(2\text{-}^t\text{BuNO})\text{-}C_6H_4CH_2\}_3N]^{3-}$ ($TriNOx^{3-}$) was developed by some of us for the stabilization of the Ce^{IV} cation.[11] This work demonstrated $[Ce^{IV}(TriNOx)]^+$ was suitable to stabilize a family of unique cerium-imido complexes—$[M(S)_x][Ce{=}NAr^F(TriNOx)]$, M = Li, K, Rb, or Cs; S = THF, TMEDA, DME, or 2.2.2-cryptand, x = 1 or 2, Ar^F = 3,5-$(CF_3)_2$-Ar, $TriNOx^{3-}$ = $[\{(2\text{-}^t\text{BuNO})C_6H_4CH_2\}_3N]^{3-}$[2d]—and enabled direct comparison with an isostructural Th^{IV} congener: $[K(S)][Th{=}NAr^F(TriNOx)]$.[9b] Theoretical studies and the relative basicity of the Ce/Th-imido group indicated a larger degree of covalency in the Ce^{IV}-imido species compared to the Th^{IV} congener. In the current work, this chemistry is extended toward isolation of the first molecular Ce^{IV}-nitride complex.

It was expected that successive deprotonation of an ammonia complex could be employed to obtain a cerium-(IV)-nitride.[5a] This strategy was previously employed for the isolation of $[M(S)_x][Ce{=}NAr^F(TriNOx)]$ and in the generation of other $RE^{III}{=}NR$ complexes RE = Sc, Y, Ce, Nd, Sm, Yb, Lu, *e.g.* $[Tp^{tBu,Me}Ln(=NAr^{iPr})(THF)_2]$, Ln = Ce, Nd, Sm.[2c,5b−d,9e,12] To initiate the synthesis, a suitable precursor was pursued: $Ce^{IV}(NH_3)(TriNOx)$. Ammonia complexes of Ce^{IV} are rare.[13] A salt metathesis reaction of $Ce^{IV}Cl(TriNOx)$ (**1**) with sodium *tetrakis*[3,5-bis-(trifluoromethyl)phenyl]borate ($NaBAr^F_4$) in CH_2Cl_2 afforded $[Ce^{IV}(TriNOx)][BAr^F_4]$, which was then subjected to anhydrous NH_3 *in situ* to form $[Ce^{IV}(NH_3)(TriNOx)][BAr^F_4]$ (**2**) in 94% isolated yield. ^{1}H NMR spectroscopy of **2** showed a broad singlet at δ = 2.86 ppm, corresponding to the characteristic $Ce^{IV}{-}NH_3$ resonance.[13] An X-ray diffraction study established the molecular structure of **2**. The Ce(1)−N(5) distance of 2.611(3) Å was similar to reported $Ce^{IV}{-}NH_3$ distances.[13] All other distances in **2** were consistent with previously reported $Ce^{IV}(TriNOx)$ complexes.[11] The IR spectrum of **2** also included a band at 3403 cm^{-1}, assigned to an N−H stretching mode.

Treating complex **2** with a toluene/diethyl ether solution (6:4 v/v) of lithium *bis*(trimethylsilyl) amide (LiHMDS) afforded black crystals in 65% yield after filtration over a Celite pad and setting the solution undisturbed at room temperature for 3 days. Following X-ray crystallography studies, the product, $[(TriNOx)Ce(Li_2\mu\text{-}N)Ce(TriNOx)][BAr^F_4]$ (**3**), was established (Scheme 2). The ^{1}H NMR spectrum of **3** shows a single pair of diastereotopic methylene protons for the $TriNOx^{3-}$ framework at δ = 4.00 and 2.35 ppm (Figure S7). The ^{7}Li NMR spectrum of **3** shows a single resonance at δ = 3.71 ppm (Figure S8).

Complex **3** is the first linear, bimetallic, crystallographically characterized lanthanide nitride complex (Figure 1). The average Ce=N bond length was 2.117(3) Å, shorter than the analogous Ce=N bond in $[Li(TMEDA)][Ce{=}NAr^F(TriNOx)]$ at 2.129(3) Å, and one of the shortest known Ce=N bonds. While **3** exhibits a formal shortness ratio (FSR = 0.909, Table S1) smaller than the previously characterized $[Li(TMEDA)][Ce{=}NAr^F(TriNOx)]$ (0.914), the structurally similar complex $[K(18\text{-crown-}6)(THF)_2][((SiMe_3)_2N)_3Th(\mu\text{-}N)Th(N(SiMe_3)_2)_3]$ exhibits a smaller FSR (0.888). This result is contrary to trends previously

Scheme 2. Synthesis of the Bridging Cerium(IV) Nitride Complex 3

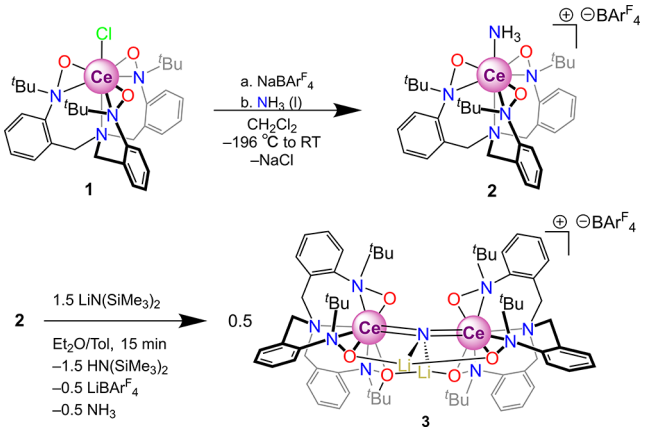

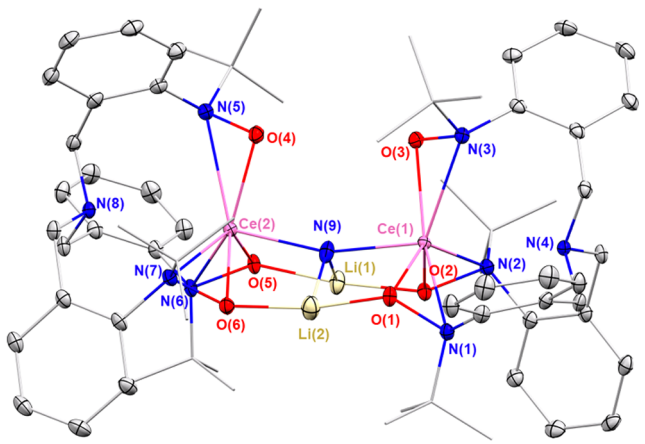

Figure 1. Thermal ellipsoid plot of **3** at 30% probability. Solvent molecules, $BAr^F_4^-$ anions, and H atoms omitted for clarity. ^{t}Bu groups depicted using a wireframe model. Selected average bond distances and bond angles for **3**: Ce−N(μ_2-nitrido) 2.117(3), Ce−O(TriNOx) 2.262(5), Ce−N(TriNOx) 2.611(5), Ce−N(bridgehead) 3.043(3), N(μ_2-nitrido)−Li 2.030(8), Ce(1)−N(9)−Ce(2) 160.53°.

observed in isostructural Ce/Th-multiple bonds.[9b] However, the capping Li-cations of **3** undoubtedly lengthen the Ce=N bonds compared to Li-free $[K(18\text{-crown-}6)(THF)_2][((SiMe_3)_2N)_3Th(\mu\text{-}N)Th(N(SiMe_3)_2)_3]$.

^{15}N-isotopic labeling was conducted to characterize **2** and **3**. Following an identical synthesis using $^{15}NH_3$ labeled: **2-^{15}N** was obtained. The ^{1}H NMR of **2-^{15}N** showed a doublet at δ = 2.88 ppm corresponding to the NH_3 protons instead of the singlet observed in **2**. A ^{15}N−^{1}H HMBC experiment on **2-^{15}N** showed a singlet in the ^{15}N NMR at δ = 25.94 ppm, downfield from an external standard of $NH_3(l)$ set at δ = 0 ppm, corresponding to the coordinated $^{15}NH_3$. The treatment of **2-^{15}N** with $Li[N(SiMe_3)_2]$ similarly produced **3-^{15}N**. Attempts to identify the ^{15}N-nitride-NMR signal for **3-^{15}N** proved unsuccessful. Confirmation of ^{15}N-labeling was achieved through acidification of **3-^{15}N**, which afforded identification of $^{15}NH_4Cl$ (Supporting Information (SI)).

Vibrational spectroscopy studies were performed to detect characteristic modes for the Ce=N=Ce unit, confirm the isotopic ^{15}N-shift, and support the assignment of the nitride in **3**. No N−H stretching bands were detected for **3**/**3-^{15}N** in their infrared spectra. The spectrum of **3** features a band at ν =

https://doi.org/10.1021/jacs.2c12145
J. Am. Chem. Soc. 2023, 145, 781−786

644 cm^{-1} corresponding to the principal Ce═N═Ce asymmetric mode. The band is shifted by −4 cm^{-1} to 640 cm^{-1} in **3**-^{15}**N** (Figure S17). Density functional theory (DFT) calculations, *vide infra*, predict the Ce═N═Ce asymmetric stretch of **3** at 680 cm^{-1} with a −12 cm^{-1} red shift in **3**-^{15}**N** (SI). A similar −7 cm^{-1} red shift was also observed with ^{15}N-enrichment in [K(18-crown-6)(THF)$_2$][((SiMe$_3$)$_2$N)$_3$Th(μ-N)Th(N(SiMe$_3$)$_2$)$_3$].[2e] The experimental and calculated Raman spectra of **3** and **3**-^{15}**N** show no noticeable isotopic shifts (Figures S21 and S22).

The solution cyclic voltammogram of **3** exhibited consecutive, reversible waves at $E_{1/2}$ = −1.54 V and −1.75 V versus Fc/Fc$^+$, assigned to successive Ce$^{IV/III}$ reductions (Figure S23). Both waves fall at more negative potentials than reported Ce^{IV}(TriNOx) complexes, including Ce^{IV}−imidos which ranged from −1.39 V to −1.41 V, highlighting strong Ce(IV) stabilization.[5a,11,14] The separation of 0.21 V between the waves suggests isolation of a mixed-valent complex may be possible. The electronic absorption spectrum of **3** showed a band at λ_{max} = 413 nm (Figure 2) that was assigned as a ligand

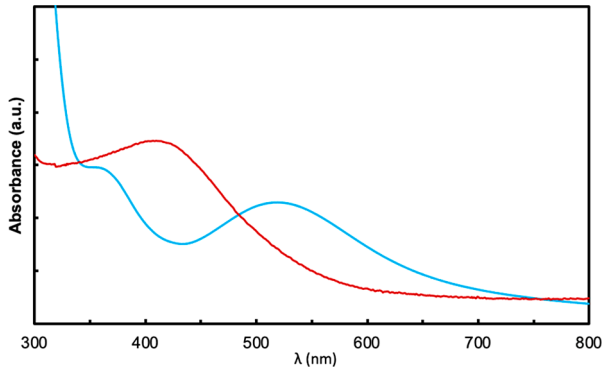

Figure 2. UV−vis spectrum of a [Li(TMEDA)][Ce═N(3,5-(CF$_3$)$_2$C$_6$H$_3$)(TriNOx)] (blue) in THF and **3** (red) in α,α,α-trifluorotoluene.

to metal (Ce 4f) charge-transfer (LMCT) transition based on the calculated spectrum (Figure S15). The more intense transitions were calculated at 394, 411, 418, and 434 nm, generating a broad nonsymmetric peak around 410 nm (Supporting Information). The transitions were assigned based on natural transition orbitals shown in Figure S28. The higher energy LMCT in **3** relative to [Li(TMEDA)][Ce═NAr^F(TriNOx)] (Figure 2) may result from stabilization of the +4 oxidation state.[5a]

The Ce L$_3$-edge XANES spectrum (Ce 2p$_{1/2}$ → 5d$_{3/2}$) of **3** contains multiple edge peaks, which is a hallmark of Ce^{IV} complexes (Figure 3).[10c,15] Two major peaks are observed at 5726 and 5736 eV, with a shoulder at ∼5719 eV and asymmetry in the first peak with tailing on the high energy side. This spectral profile is reminiscent of those observed for Ce^{IV}-imido complexes supported by TriNOx^{3-} ligands,[9e] the most notable difference being an increase in the relative intensity of the Ce^{III} and Ce^{IV} peaks (Figure S26). These peaks are often assigned using a configuration interaction model involving 4f^0 and 4f^1$\underline{L}$ ground-state configurations, where $\underline{L}$ represents a ligand hole resulting from LMCT. According to this model,[15a,16] the large peak-to-peak splitting (10 eV) between configurations arises in the excited state from differences in the number of 4f electrons available to screen the 5d electrons from the Ln 2p core-hole. The low energy peak is thus

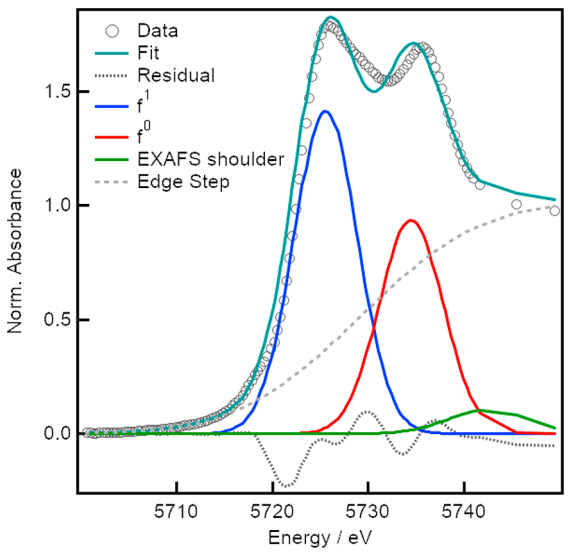

Figure 3. Ce L$_{III}$-edge XANES spectrum of **3**, characteristic of formally Ce^{IV} complexes. See Supporting Information for fitting details.

attributed to the 4f^1$\underline{L}$5d^1 (or Ce^{III}) configuration, and the higher energy peak is attributed to the 4f^{0}5d^1 (or Ce^{IV}) configuration. Their relative weights were evaluated using established curve-fitting methods,[9e] which indicated that the 4f^{0}5d^1 configuration had a relative weight of 0.40(3). After accounting for error, this value is statistically equivalent to those found previously for TriNOx^{3-} systems using the same curve-fitting method, despite the appearance of an increase in Ce^{III} character for **3** by visual inspection of the experimental spectra (Figure S26).[9e] Hence, the XANES results support an electronic structure assignment for **3** that is typical for cerium(IV) complexes, in that the Ce center has a formal +4 charge that is modulated by donation bonding.[10c]

To further understand the electronic structure of the Ce═N═Ce subsystem in **3**, DFT calculations were performed with the B3LYP functional, and small-core Stuttgart energy-consistent relativistic pseudopotentials.[17] Additional calculated benchmark data are provided in the SI, showing that the results are not strongly dependent on the chosen functional. DFT was presumed a suitable approach, given that spectroscopic results supported purely Ce(IV) character in Ce═N═Ce. Indeed, good agreement between optimized and experimental structural parameters for **3** (Table S3) was obtained, with calculated Ce−N (μ$_2$-nitrido and TriNOx) and Ce−O (TriNOx) distances within 0.02 Å of experimental X-ray crystal structure data.

The metal−ligand bonding in **3** was analyzed in terms of natural localized molecular orbitals (NLMOs). As seen in Figure 4 and Table S4, the Ce═N═Ce interactions feature two N → Ce 2-center-2-electron (2c-2e) σ-donation bonds, accompanied by two N → Ce three-center-2-electron π-donation interactions. As expected for dative interactions, the bonds are polarized toward N. Overall, there is double bond character for each Ce═N interaction, confirmed by the Wiberg bond orders exceeding 1 (1.21 on average). The Ce−N σ-bonds in **3** have 16% Ce weight (57% 5d, 40% 4f), and the Ce−N three-center π-bonds each have 11% Ce weight (53% 5d, 47% 4f) (Table S4), showing a strong involvement of the cerium 4f shell. The Ce═N═Ce moiety exhibits similar covalency as the Ce═N bond in the previously reported

https://doi.org/10.1021/jacs.2c12145
J. Am. Chem. Soc. 2023, 145, 781−786

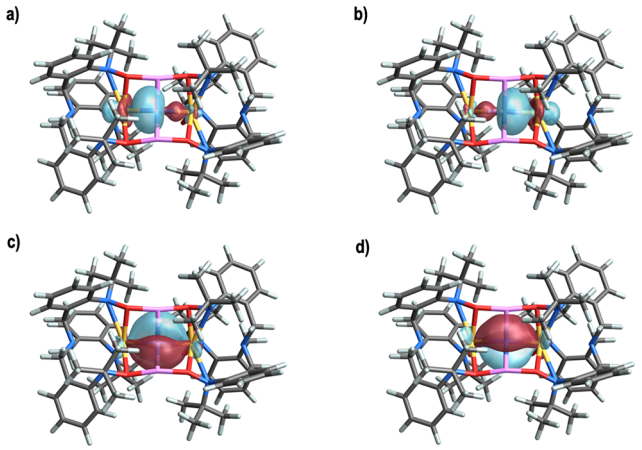

Figure 4. Isosurface plots (±0.03 au) of σ-bonding (a,b) and π-bonding (c,d) localized orbitals (NLMOs) of the Ce═N═Ce fragment of **3**.

[Li(TMEDA)][Ce═NAr^{F}(TriNOx)] [Scheme 1, with Ce−N σ-bonds comprising 11% Ce weight (65% 5d, 29% 4f) and Ce−N π-bonds comprising 17% Ce weight (50% 5d, 50% 4f)], as well as the bonds in the Th═N═Th moiety of [K(18-crown-6)(THF)$_2$][((SiMe$_3$)$_2$N)$_3$Th(μ-N)Th(N(SiMe$_3$)$_2$)$_3$] [with 10% Th weight (67% 6d, 24% 5f) in the Th−N σ-bonds and 16% Th weight (58% 6d, 42% 5f) in the Th−N π-bonds]. The remaining σ-interactions of Ce with the N and O atoms of the TriNOx ligands are less covalent, with ∼5−9% Ce-weight (Figure S27). Overall, Ce receives considerable electron donation from the surrounding ligands: the calculated Ce natural charge of +1.8 is much below the formal +4 charge. The Ce natural electron configuration assigned by the calculation is 4f$^{0.98}$5d$^{1.21}$, deviating strongly from the formal 4f^{0}5d^0. The size of the complex and low local symmetry of the Ce centers prohibited L_{III}-edge wave function calculations.[10c,18] But, the XANES data and computational results are consistent with a formal and spectroscopic oxidation state of purely cerium(IV) for **3**, implying a *bona fide* N^{3-} moiety.

To summarize, a bimetallic, tetravalent cerium complex featuring a Ce═N═Ce moiety was isolated. The μ_2-nitrido is stabilized by the coordination of two Li cations and the steric bulk of the TriNOx^{3-} ligand framework. DFT calculations supported double bonds in the Ce═N═Ce fragment of **3** and strong participation of Ce in both σ- and π-bonding. These results are important for further exploration of metal−ligand multiple bonding of f-elements and investigation into their electronic structure.

■ ASSOCIATED CONTENT

Supporting Information

The Supporting Information is available free of charge at https://pubs.acs.org/doi/10.1021/jacs.2c12145.

Experimental procedures, spectroscopic data, computational details, and crystallographic data for **2** and **3** (PDF)

Accession Codes

CCDC 2193120−2193121 contain the supplementary crystallographic data for this paper. These data can be obtained free of charge via www.ccdc.cam.ac.uk/data_request/cif, or by emailing data_request@ccdc.cam.ac.uk, or by contacting The Cambridge Crystallographic Data Centre, 12 Union Road, Cambridge CB2 1EZ, UK; fax: +44 1223 336033.

■ AUTHOR INFORMATION

Corresponding Authors

Stefan G. Minasian − *Lawrence Berkeley National Laboratory, Berkeley, California 94720, United States;* orcid.org/0000-0003-1346-7497; Email: sgminasian@lbl.gov

Jochen Autschbach − *Department of Chemistry, University of Buffalo, Buffalo, New York 14260, United States;* orcid.org/0000-0001-9392-877X; Email: jochena@buffalo.edu

Eric J. Schelter − *P. Roy and Diana T. Vagelos Laboratories, Department of Chemistry, University of Pennsylvania, Philadelphia, Pennsylvania 19104, United States;* orcid.org/0000-0002-8143-6206; Email: schelter@sas.upenn.edu

Authors

Henry H. Wilson − *P. Roy and Diana T. Vagelos Laboratories, Department of Chemistry, University of Pennsylvania, Philadelphia, Pennsylvania 19104, United States*

Xiaojuan Yu − *Department of Chemistry, University of Buffalo, Buffalo, New York 14260, United States;* orcid.org/0000-0001-9412-6170

Thibault Cheisson − *P. Roy and Diana T. Vagelos Laboratories, Department of Chemistry, University of Pennsylvania, Philadelphia, Pennsylvania 19104, United States;* Present Address: Dr. T. Cheisson: Eramet Ideas, 1 rue Albert Einstein, 78190, Trappes, France; orcid.org/0000-0003-4359-5115

Patrick W. Smith − *Lawrence Berkeley National Laboratory, Berkeley, California 94720, United States;* orcid.org/0000-0001-5575-4895

Pragati Pandey − *P. Roy and Diana T. Vagelos Laboratories, Department of Chemistry, University of Pennsylvania, Philadelphia, Pennsylvania 19104, United States;* orcid.org/0000-0003-0032-7364

Patrick J. Carroll − *P. Roy and Diana T. Vagelos Laboratories, Department of Chemistry, University of Pennsylvania, Philadelphia, Pennsylvania 19104, United States;* orcid.org/0000-0002-8142-7211

Complete contact information is available at: https://pubs.acs.org/10.1021/jacs.2c12145

Author Contributions

[||]T.C. and X.Y. contributed equally to this work.

Notes

The authors declare no competing financial interest.

■ ACKNOWLEDGMENTS

E.J.S. thanks the National Science Foundation (CHE-1955724) for the support of this work. E.J.S. also gratefully acknowledges the Office of Basic Energy Sciences, Chemical Sciences, Geosciences and Biosciences Division, Heavy Element Chemistry Program, of the U.S. Department of Energy under Award DE-SC0020169 for support of P.P. We also thank the Jasco Center at the University of Pennsylvania for providing access to Raman spectrometry resources. J.A. acknowledges support for the theoretical component of this

study by DOE award DE-SC0020169. We thank the Center for Computational Research (CCR) at the University of Buffalo for providing computational resources. Work at Lawrence Berkeley National Laboratory was supported by the Director, Office of Science, Office of Basic Energy Sciences, Division of Chemical Sciences, Geosciences, and Biosciences Heavy Element Chemistry Program of the U.S. Department of Energy (DOE) at LBNL under Contract No. DE-AC02-05CH11231. XANES measurements were performed at beamline 11-2 at the Stanford Synchrotron Radiation Lightsource, which is supported by the U.S. Department of Energy, Office of Science, Office of Basic Energy Sciences under Contract No. DE-AC02-76SF00515.

REFERENCES

(1) (a) Cummins, C. C.; Baxter, S. M.; Wolczanski, P. T. Methane and Benzene Activation Via Transient (Tert-Bu3sinh)2zr = Nsi-Tert-Bu3. *J. Am. Chem. Soc.* **1988**, *110* (26), 8731−8733. (b) Hazari, N.; Mountford, P. Reactions and applications of titanium imido complexes. *Acc. Chem. Res.* **2005**, *38* (11), 839−849. (c) Jia, H. P.; Quadrelli, E. A. Mechanistic aspects of dinitrogen cleavage and hydrogenation to produce ammonia in catalysis and organometallic chemistry: relevance of metal hydride bonds and dihydrogen. *Chem. Soc. Rev.* **2014**, *43* (2), 547−564. (d) Kriegel, B. M.; Bergman, R. G.; Arnold, J. Nitrene Metathesis and Catalytic Nitrene Transfer Promoted by Niobium Bis(imido) Complexes. *J. Am. Chem. Soc.* **2016**, *138* (1), 52−55. (e) Masero, F.; Perrin, M. A.; Dey, S.; Mougel, V. Dinitrogen Fixation: Rationalizing Strategies Utilizing Molecular Complexes. *Chem.—Eur. J.* **2021**, *27* (12), 3892−3928. (f) Thompson, N. B.; Green, M. T.; Peters, J. C. Nitrogen Fixation via a Terminal Fe(IV) Nitride. *J. Am. Chem. Soc.* **2017**, *139* (43), 15312−15315.

(2) (a) Camp, C.; Pecaut, J.; Mazzanti, M. Tuning Uranium-Nitrogen Multiple Bond Formation with Ancillary Siloxide Ligands. *J. Am. Chem. Soc.* **2013**, *135* (32), 12101−12111. (b) Fox, A. R.; Arnold, P. L.; Cummins, C. C. Uranium Nitrogen Multiple Bonding: Isostructural Anionic, Neutral, and Cationic Uranium Nitride Complexes Featuring a Linear U = N=U Core. *J. Am. Chem. Soc.* **2010**, *132* (10), 3250−3251. (c) Gordon, J. C.; Giesbrecht, G. R.; Clark, D. L.; Hay, P. J.; Keogh, D. W.; Poli, R.; Scott, B. L.; Watkin, J. G. The first example of a mu(2)-imido functionality bound to a lanthanide metal center: X-ray crystal structure and DFT study of [(mu-ArN)Sm(mu-NHAr)(mu-Me)AlMe2](2) (Ar = 2,6-(Pr2C6H3)-Pr-i). *Organometallics* **2002**, *21* (22), 4726−4734. (d) Solola, L. A.; Zabula, A. V.; Dorfner, W. L.; Manor, B. C.; Carroll, P. J.; Schelter, E. J. An Alkali Metal-Capped Cerium(IV) Imido Complex. *J. Am. Chem. Soc.* **2016**, *138* (22), 6928−6931. (e) Staun, S. L.; Sergentu, D. C.; Wu, G.; Autschbach, J.; Hayton, T. W. Use of N-15 NMR spectroscopy to probe covalency in a thorium nitride. *Chem. Sci.* **2019**, *10* (26), 6431−6436. (f) Fox, A. R.; Cummins, C. C. Uranium-Nitrogen Multiple Bonding: The Case of a Four-Coordinate Uranium(VI) Nitridoborate Complex. *J. Am. Chem. Soc.* **2009**, *131* (16), 5716−5717. (g) King, D. M.; Cleaves, P. A.; Wooles, A. J.; Gardner, B. M.; Chilton, N. F.; Tuna, F.; Lewis, W.; McInnes, E. J. L.; Liddle, S. T. Molecular and electronic structure of terminal and alkali metal-capped uranium(V) nitride complexes. *Nat. Commun.* **2016**, *7*, 13773.

(3) Sergentu, D. C.; Kent, G. T.; Staun, S. L.; Yu, X. J.; Cho, H.; Autschbach, J.; Hayton, T. W. Probing the Electronic Structure of a Thorium Nitride Complex by Solid-State ^{15}N NMR Spectroscopy. *Inorg. Chem.* **2020**, *59* (14), 10138−10145.

(4) (a) Falcone, M.; Chatelain, L.; Scopelliti, R.; Zivkovic, I.; Mazzanti, M. Nitrogen reduction and functionalization by a multimetallic uranium nitride complex. *Nature* **2017**, *547* (7663), 332−335. (b) Hayton, T. W. Recent developments in actinide-ligand multiple bonding. *Chem. Commun.* **2013**, *49* (29), 2956−2973. (c) King, D. M.; Tuna, F.; McInnes, E. J. L.; McMaster, J.; Lewis, W.; Blake, A. J.; Liddle, S. T. Synthesis and Structure of a Terminal Uranium Nitride Complex. *Science* **2012**, *337* (6095), 717−720. (d) Mullane, K. C.; Ryu, H.; Cheisson, T.; Grant, L. N.; Park, J. Y.; Manor, B. C.; Carroll, P. J.; Baik, M. H.; Mindiola, D. J.; Schelter, E. J. C-H Bond Addition across a Transient Uranium-Nitrido Moiety and Formation of a Parent Uranium Imido Complex. *J. Am. Chem. Soc.* **2018**, *140* (36), 11335−11340. (e) Schadle, D.; Anwander, R. Rare-earth metal and actinide organoimide chemistry. *Chem. Soc. Rev.* **2019**, *48* (24), 5752−5805.

(5) (a) Solola, L. A.; Zabula, A. V.; Dorfner, W. L.; Manor, B. C.; Carroll, P. J.; Schelter, E. J. Cerium(IV) Imido Complexes: Structural, Computational, and Reactivity Studies. *J. Am. Chem. Soc.* **2017**, *139* (6), 2435−2442. (b) Rieser, T. E.; Thim-Sporing, R.; Schadle, D.; Sirsch, P.; Litlabo, R.; Tornroos, K. W.; Maichle-Mossmer, C.; Anwander, R. Open-Shell Early Lanthanide Terminal Imides. *J. Am. Chem. Soc.* **2022**, *144* (9), 4102−4113. (c) Schadle, D.; Meermann-Zimmermann, M.; Schadle, C.; Maichle-Mossmer, C.; Anwander, R. Rare-Earth Metal Complexes with Terminal Imido Ligands. *Eur. J. Inorg. Chem.* **2015**, *2015* (8), 1334−1339. (d) Lu, E. L.; Li, Y. X.; Chen, Y. F. A scandium terminal imido complex: synthesis, structure and DFT studies. *Chem. Commun.* **2010**, *46* (25), 4469−4471.

(6) (a) Giesbrecht, G. R.; Gordon, J. C. Lanthanide alkylidene and imido complexes. *Dalton Trans* **2004**, No. 16, 2387−2393. (b) Summerscales, O. T.; Gordon, J. C. Complexes containing multiple bonding interactions between lanthanoid elements and main-group fragments. *Rsc Adv.* **2013**, *3* (19), 6682−6692. (c) Raymond, K. N.; Eigenbrot, C. W. Structural Criteria for the Mode of Bonding of Organoactinides and Organolanthanides and Related-Compounds. *Acc. Chem. Res.* **1980**, *13* (8), 276−283.

(7) Zhang, Y.; Schiemenz, S.; Popov, A. A.; Dunsch, L. Strain-Driven Endohedral Redox Couple Ce-IV/Ce-III in Nitride Clusterfullerenes CeM2N@C-80 (M = Sc, Y, Lu). *J. Phys. Chem. Lett.* **2013**, *4* (15), 2404−2409.

(8) (a) Willson, S. P.; Andrews, L. Characterization of the reaction products of laser-ablated early lanthanide metal atoms with dinitrogen. Infrared spectra of LnN, LnN(2), (LnN)(2), and Ln(NN)(x) molecules. *J. Phys. Chem. A* **1998**, *102* (50), 10238−10249. (b) Willson, S. P.; Andrews, L.; Neurock, M. Characterization of the reaction products of laser-ablated lanthanide metal atoms with nitric oxide. Infrared spectra of the NLnO molecules in solid argon. *J. Phys. Chem. A* **2000**, *104* (16), 3446−3456.

(9) (a) Cantat, T.; Graves, C. R.; Jantunen, K. C.; Burns, C. J.; Scott, B. L.; Schelter, E. J.; Morris, D. E.; Hay, P. J.; Kiplinger, J. L. Evidence for the Involvement of 5f Orbitals in the Bonding and Reactivity of Organometallic Actinide Compounds: Thorium(IV) and Uranium-(IV) Bis(hydrazonato) Complexes. *J. Am. Chem. Soc.* **2008**, *130* (51), 17537−17551. (b) Cheisson, T.; Kersey, K. D.; Mahieu, N.; McSkimming, A.; Gau, M. R.; Carroll, P. J.; Schelter, E. J. Multiple Bonding in Lanthanides and Actinides: Direct Comparison of Covalency in Thorium(IV)- and Cerium(IV)-Imido Complexes. *J. Am. Chem. Soc.* **2019**, *141* (23), 9185−9190. (c) Gardner, B. M.; Cleaves, P. A.; Kefalidis, C. E.; Fang, J.; Maron, L.; Lewis, W.; Blake, A. J.; Liddle, S. T. The role of 5f-orbital participation in unexpected inversion of the sigma-bond metathesis reactivity trend of triamidoamine thorium(IV) and uranium(IV) alkyls. *Chem. Sci.* **2014**, *5* (6), 2489−2497. (d) Kent, G. T.; Yu, X. J.; Pauly, C.; Wu, G.; Autschbach, J.; Hayton, T. W. Synthesis of Parent Acetylide and Dicarbide Complexes of Thorium and Uranium and an Examination of Their Electronic Structures. *Inorg. Chem.* **2021**, *60* (20), 15413−15420. (e) Moreau, L. M.; Lapsheva, E.; Amaro-Estrada, J. I.; Gau, M. R.; Carroll, P. J.; Manor, B. C.; Qiao, Y. S.; Yang, Q. M.; Lukens, W. W.; Sokaras, D.; et al. Electronic structure studies reveal 4f/5d mixing and its effect on bonding characteristics in Ce-imido and -oxo complexes. *Chem. Sci.* **2022**, *13* (6), 1759−1773.

(10) (a) Halbach, R. L.; Nocton, G.; Booth, C. H.; Maron, L.; Andersen, R. A. Cerium Tetrakis(tropolonate) and Cerium Tetrakis-(acetylacetonate) Are Not Diamagnetic but Temperature-Independent Paramagnets. *Inorg. Chem.* **2018**, *57* (12), 7290−7298. (b) Booth, C. H.; Walter, M. D.; Daniel, M.; Lukens, W. W.; Andersen, R. A.

https://doi.org/10.1021/jacs.2c12145
J. Am. Chem. Soc. 2023, 145, 781−786

Self-contained Kondo effect in single molecules. *Phys. Rev. Lett.* **2005**, *95* (26), 267202. (c) Sergentu, D. C.; Booth, C. H.; Autschbach, J. Probing Multiconfigurational States by Spectroscopy: The Cerium XAS L-3-edge Puzzle. *Chem.—Eur. J.* **2021**, *27* (25), 7239−7251. (d) Walter, M. D.; Booth, C. H.; Lukens, W. W.; Andersen, R. A. Cerocene Revisited: The Electronic Structure of and Interconversion Between Ce-2(C8H8)(3) and Ce(C8H8)(2). *Organometallics* **2009**, *28* (3), 698−707.

(11) Bogart, J. A.; Lippincott, C. A.; Carroll, P. J.; Booth, C. H.; Schelter, E. J. Controlled Redox Chemistry at Cerium within a Tripodal Nitroxide Ligand Framework. *Chem.—Eur. J.* **2015**, *21* (49), 17850−17859.

(12) (a) Chan, H. S.; Li, H. W.; Xie, Z. W. Synthesis and structural characterization of imido-lanthanide complexes with a metal-nitrogen multiple bond. *Chem. Commun.* **2002**, No. 6, 652−653. (b) Chu, T.; Piers, W. E.; Dutton, J. L.; Parvez, M. Synthesis and Reactivity of a Terminal Scandium Imido Complex. *Organometallics* **2013**, *32* (5), 1159−1165. (c) Lu, E.; Chu, J. X.; Chen, Y. F. Scandium Terminal Imido Chemistry. *Acc. Chem. Res.* **2018**, *51* (2), 557−566. (d) Wicker, B. F.; Fan, H. J.; Hickey, A. K.; Crestani, M. G.; Scott, J.; Pink, M.; Mindiola, D. J. Evidence for the Existence of Terminal Scandium Imidos: Mechanistic Studies Involving Imido-Scandium Bond Formation and C-H Activation Reactions. *J. Am. Chem. Soc.* **2012**, *134* (49), 20081−20096. (e) Patrick, E. A.; Yang, Y.; Piers, W. E.; Maron, L.; Gelfand, B. S. A monoanionic pentadentate ligand platform for scandium-pnictogen multiple bonds. *Chem. Commun.* **2021**, *57* (69), 8640−8643. (f) Knight, L. K.; Piers, W. E.; Fleurat-Lessard, P.; Parvez, M.; McDonald, R. beta-diketiminato scandium chemistry: Synthesis, characterization, and thermal behavior of primary amido alkyl derivatives. *Organometallics* **2004**, *23* (9), 2087−2094. (g) Wen, Q. Q.; Rajeshkumar, T.; Maron, L.; Leng, X. B.; Chen, Y. F. Synthesis, Characterization, and Reactivity of a Hydrido- and Imido-Bridged Dinuclear Ytterbium(III) Complex. *Angew. Chem. Int. Ed.* **2022**, *61* (25), No. e202200540.

(13) Friedrich, J.; Maichle-Mossmer, C.; Schrenk, C.; Schnepf, A.; Anwander, R. Ceric Ammonium Nitrate and Ceric Ammonium Chloride as Precursors for Ceric Siloxides: Ammonia and Ammonium Inclusion. *Eur. J. Inorg. Chem.* **2019**, *2019* (1), 79−90.

(14) Bogart, J. A.; Lewis, A. J.; Medling, S. A.; Piro, N. A.; Carroll, P. J.; Booth, C. H.; Schelter, E. J. Homoleptic Cerium(III) and Cerium(IV) Nitroxide Complexes: Significant Stabilization of the 4+Oxidation State. *Inorg. Chem.* **2013**, *52* (19), 11600−11607.

(15) (a) Kaindl, G.; Schmiester, G.; Sampathkumaran, E. V.; Wachter, P. Pressure-Induced Changes in Liii X-Ray-Absorption near-Edge Structure of CeO_2 and CeF_4 - Relevance to 4f-Electronic Structure. *Phys. Rev. B* **1988**, *38* (14), 10174−10177. (b) Loble, M. W.; Keith, J. M.; Altman, A. B.; Stieber, S. C. E.; Batista, E. R.; Boland, K. S.; Conradson, S. D.; Clark, D. L.; Pacheco, J. L.; Kozimor, S. A.; et al. Covalency in Lanthanides. An X-ray Absorption Spectroscopy and Density Functional Theory Study of LnCl(6)(x-) (x = 3, 2). *J. Am. Chem. Soc.* **2015**, *137* (7), 2506−2523. (c) Minasian, S. G.; Batista, E. R.; Booth, C. H.; Clark, D. L.; Keith, J. M.; Kozimor, S. A.; Lukens, W. W.; Martin, R. L.; Shuh, D. K.; Stieber, S. C. E.; et al. Quantitative Evidence for Lanthanide-Oxygen Orbital Mixing in CeO2, PrO2, and TbO2. *J. Am. Chem. Soc.* **2017**, *139* (49), 18052−18064.

(16) (a) Kas, J. J.; Rehr, J. J.; Curtis, J. B. Particle-hole cumulant approach for inelastic losses in x-ray spectra. *Phys. Rev. B* **2016**, *94* (3), 035156. (b) Kotani, A.; Kvashnina, K. O.; Butorin, S. M.; Glatzel, P. Spectator and participator processes in the resonant photon-in and photon-out spectra at the Ce L-3 edge of CeO2. *Eur. Phys. J. B* **2012**, *85* (8), 257. (c) Sham, T. K.; Gordon, R. A.; Heald, S. M. Resonant inelastic X-ray scattering at the Ce L-3 edge of $CePO_4$ and CeO_2: Implications for the valence of CeO_2 and related phenomena. *Phys. Rev. B* **2005**, *72* (3), 035113.

(17) (a) Frisch, M. J.; Trucks, G. W.; Schlegel, H. B.; Scuseria, G. E.; Robb, M. A.; Cheeseman, J. R.; Scalmani, G.; Barone, V.; Petersson, G. A.; Nakatsuji, H. *Gaussian 16, Revision A.03*; Gaussian Inc.: Wallingford, CT; 2016. (b) Becke, A. D. Density-Functional Exchange-Energy Approximation with Correct Asymptotic Behavior. *Phys. Rev. A* **1988**, *A38*, 3098. (c) Lee, C. T.; Yang, W. T.; Parr, R. G. Development of the Colle-Salvetti Correlation-Energy Formula into a Functional of the Electron Density. *Phys. Rev.* **1988**, *B37*, 785. (d) Cao, X. Y.; Dolg, M. Valence basis sets for relativistic energy-consistent small-core lanthanide pseudopotentials. *J. Chem. Phys.* **2001**, *115* (16), 7348−7355.

(18) Sergentu, D. C.; Autschbach, J. X-ray absorption spectra of f-element complexes: insight from relativistic multiconfigurational wavefunction theory. *Dalton Trans.* **2022**, *51* (5), 1754−1764.

https://doi.org/10.1021/jacs.2c12145
J. Am. Chem. Soc. 2023, 145, 781−786